Mechanical, Dynamic Thermal Mechanical, and Creep Properties of Hot-Pressed Wood-Plastic Composites

Yan Cao,[a,b,#] Baoyu Liu,[a,#] Guangping Deng,[a] Xueshan Hua,[c] Liling Wei,[a] Xiaohui Yang,[a] Hailong Xu,[c,*] and Lifen Li [d,*]

To investigate the influence of reinforced fiber size on the service performance of wood-plastic composites (WPCs), high-density polyethylene (HDPE) composites were prepared using poplar fibers of seven different sizes. Their bending and impact properties, dynamic thermal mechanical properties, and 24 h creep-24 h recovery performance were analyzed. The WPCs reinforced with 80 to 120 mesh fibers had the worst mechanical properties. The WPCs reinforced with 10 to 120 mesh fibers had the highest bending strength, reaching 28.1 MPa, while WPCs reinforced with 20 to 40 mesh fibers had the greatest bending modulus of 2.73 GPa. The WPCs with 20 to 80 mesh fibers had the highest impact strength, reaching 7.75 kJ/m^2. Excessively large or small fiber sizes did not benefit the mechanical properties of WPCs. As the temperature increased, the storage modulus of WPCs decreased. Additionally, as the mesh size of wood fibers increased, the loss modulus increased, while the loss tangent gradually decreased, resulting in reduced toughness and more pronounced elastic behavior. Under a 50 N load, WPCs with the mixed mesh fiber outperformed WPCs with single mesh fibers in 24 h creep performance, WPCs reinforced with 20 to 80 mesh fiber showing the best creep resistance.

DOI: 10.15376/biores.21.1.1564-1582

Keywords: Wood-plastic composites; Mechanical properties; Dynamic thermal mechanical properties; Creep properties

*Contact information: a: Special and Key Laboratory for Development and Utilization of Guizhou Superior Bio-Based Materials, Guizhou Minzu University, Guiyang 550025, Guizhou, China; b: Engineering Research Center of Green and Low-carbon Technology for Plastic Application, Guizhou Minzu University, Guiyang, 550025, Guizhou, China; c: College of Data Science and Information Engineering, Guizhou Minzu University, Guiyang, Guizhou, 550025, China; d: College of Forestry, Guizhou University, Guiyang 550025, Guizhou, China; *Corresponding author: xu00hailong@163.com; lifenli2011@163.com*

INTRODUCTION

Wood-plastic composites (WPCs) are renewable composites made by combining waste plant fibers with polymer materials, which include wood chips, rice husks, and straw, with polymer matrices, mainly polyethylene, polypropylene, and polyvinyl chloride (Ribeiro *et al*. 2023; Ye *et al*. 2023; Khamtree *et al*. 2024; Hassona *et al*. 2025; Cao *et al*. 2025). The lignocellulosic fibers in these composites are typically sourced from agricultural waste or forestry processing residues, while the plastics are mostly recycled waste plastics. Therefore, the production of WPCs itself achieves the reuse of waste resources, aligning with the concept of sustainable development (Jeon *et al*. 2024; Mital'ová *et al*. 2024; Qi *et al*. 2024).

The renewability of WPCs lies in both the recyclability of their raw materials and the recyclability of their products. WPCs have excellent recyclability, with their waste being 100% recyclable and reproduced into new WPC products. This characteristic ensures that WPCs do not become an environmental burden at the end of their life cycle, but can continue to play a role in the circular economy. Recycled WPCs can be reprocessed at a low cost to create new products or components, which helps reduce production costs for manufacturers and broadens the potential application of WPCs. WPCs can facilitate modular customization and quick assembly. This not only meets the requirements of prefabricated buildings, but it also ensures controllable construction periods, reduced working hours, and lower construction costs. These characteristics make WPCs a versatile and efficient material choice in the construction industry. The recyclability of WPCs highlights their environmental friendliness. Through serving as alternatives to traditional wood and plastic products, WPCs help conserve forest resources and reduce environmental pollution. At the same time, during the production process, various additives, such as flame retardants, antimicrobial agents, and UV stabilizers, can be incorporated to enhance their performance, including flame resistance, antibacterial properties, and weathering resistance. The recyclability and environmental friendliness of WPCs have led to a wide range of applications in a number of fields, such as construction, furniture, and logistics packaging. For example, in the construction industry, WPCs can be used to manufacture exterior wall panels, ceiling panels, decorative wall panels, *etc*. In the furniture industry, they can be used for manufacturing integrated cabinets, wardrobes, *etc*. In the logistics packaging industry, they can be used for manufacturing transport pallets, *etc*.

There are many factors that affect the mechanical properties of WPCs, including the type of polymeric matrix (Ratanawilai and Taneerat 2018; Na *et al*. 2022; Xue *et al*. 2024; Nuruzzaman *et al*. 2025), the amount of wood fiber added (Barbos *et al*. 2020; Yang *et al*. 2025), the species of wood fiber (Kim *et al*. 2009; Mu *et al*. 2018; Zhao *et al*. 2024), the particle size of the wood fiber, processing parameters, and interphase modification (Aref *et al*. 2018; Ayana *et al*. 2025), *etc*. Bouafif *et al.* (2009) investigated the effect of wood fiber size on the physical and mechanical properties of WPCs. They found that while the fiber size had no significant effect on the water absorption rate of the composites, it significantly impacted their mechanical properties. Moreover, an increase in fiber size improved the tensile and flexural strengths, as well as the modulus of the composites. For instance, in cases with higher fiber content (45 wt%), when the fiber size increased from 65 mesh to 24 mesh, the flexural strength of the composites increased approximately 24%. Similarly, Chaudemanche *et al.* (2018) found that within the same size range, coarse wood flour was less damaged and showed a higher aspect ratio compared to fine wood flours. Moreover, as the size of the wood fibers increased, the bending strength of the composites also improved. This phenomenon can be explained by a better distribution of polymers and additives around the fibers compared to smaller fibers.

Research has demonstrated that the type and content of compatibilizers play a crucial role in determining the mechanical properties of WPCs. Mustafa *et al*. (2024) compared the effects of two coupling agents, maleic anhydride-grafted polypropylene (MAPP) and maleic anhydride-grafted polyethylene (MAPE), on the properties of wood fiber/polypropylene composites. Their findings indicated that the type of coupling agent significantly affected the mechanical properties of the composites. Specifically, the addition of MAPP increased the tensile strength and flexural strength of the composites by 13% and 18%, respectively, whereas MAPE treatment led to more substantial improvements of 74% and 60% in these properties. Rao *et al*. (2018) explained that MAPE

not only forms chemical bonds with wood fibers through its active groups but also entangles with the non-polar polyethylene matrix at the molecular level, thereby significantly improving the fiber-matrix interfacial adhesion. In addition, the research by Xu *et al*. (2024) indicated that as the proportion of MAPE increases, the creep resistance of WPCs initially increases and then decreases.

Research on dynamic thermal mechanical properties of WPCs can reveal their mechanical response under varying temperatures and frequencies. Through dynamic mechanical tests, parameters such as the storage modulus, loss modulus, and loss tangent, of WPCs can be obtained. These parameters reflect the energy storage, dissipation, and damping characteristics of the WPCs during force application, and enable the identification of key factors affecting the storage modulus, glass transition temperature, and other properties of WPCs. This is crucial for a deeper understanding of the mechanical properties and performance behavior of WPCs under different conditions, thus providing a scientific basis for their application in specific fields. For example, in environments requiring high temperatures or high-frequency vibrations, WPCs with excellent dynamic thermal mechanical properties will be more competitive (Xu *et al*. 2023).

Creep is a phenomenon in which the deformation of a material gradually increases with time under the action of a constant external force at a certain temperature. For WPCs, creep performance under short- and long-term loading is one of their important mechanical properties (Ratanawilai and Srivabut 2022). Creep can significantly affect their durability and normal service life when used as engineering materials (such as beams, columns, trusses, flooring, floor panels, and other building components, as well as vehicles frames, doors and windows, outdoor walkways, bridges, and sleepers). The study of creep performance can reveal the viscoelastic mechanisms of WPCs, which can help to understand the deformation patterns of WPCs under long-term stress, provide a scientific basis for the rational application of WPCs, and provide theoretical guidance for the design, production, and use of WPCs. This knowledge assists engineers and designers in selecting and using materials more effectively to prevent safety hazards during application (Xue *et al*. 2024).

Poplar is one of the most important forest trees in eastern China. It is known for its fast-growing rate, its ease of vegetative propagation and transformation, and its high economic value. In the process of poplar wood processing, a large amount of waste with different particle sizes will be produced, and the use of these wastes to prepare WPCs has not only good economic benefits, but also significant ecological benefits. Whether poplar residues need to be screened or can be used directly will affect the complexity of WPCs fabrication. In addition, research on the effects of fiber size on WPCs performance—especially on dynamic thermal mechanical properties and creep-recovery behavior—remains limited. Therefore, this study employed a completely randomized experimental design with repeated experiments across seven treatment groups, which differed in fiber size composition, to systematically investigate how poplar fiber size composition affects the mechanical properties (including bending strength and impact resistance), dynamic thermal mechanical characteristics, and 24 h creep- 24 h recovery behavior of the HDEP-based WPCs. This investigation not only helps to improve the comprehensive performance and application value of WPCs, but also promotes the rapid development of new materials industry and the progress of environmental protection.

EXPERIMENTAL

Material Preparation

Poplar (*Populus alba* L.) fibers or particles were crushed (FZ-102 electric animal and plant pulverizer, Tianjin Testing Instruments Co., Ltd.) and screened into four mesh sizes, which were denoted by the letters A, B, C, and D for convenience of description. Among them, A represents 80 to 120 mesh (125 to 180 μm) poplar fibers, B represents 40 to 80 mesh (180 to 425 μm) poplar fibers, C represents 20 to 40 mesh (425 to 850 μm) poplar fibers, and D corresponds to 10 to 20 mesh (850 to 2000 μm) poplar fibers.

The wood fibers of different mesh sizes were observed by stereomicroscope (XTL-350Z, Shanghai Changfang Optical Instruments Co., Ltd.). Figure 1 shows the magnification effect of 33 times of wood fiber, which can be clearly seen that with the decrease of fiber mesh size, the size of the fiber gradually increases. The 10 to 20 mesh fibers (d) were rod-shaped, while the 80 to 120 mesh fibers (a) were powdery.

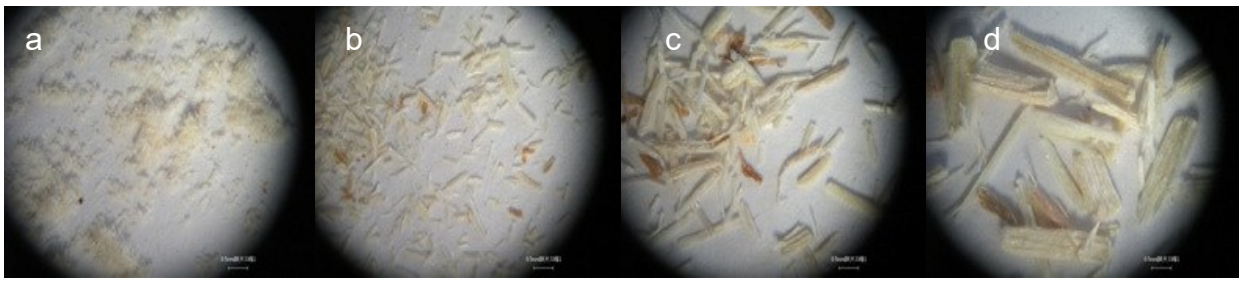

Fig. 1. Surface of wood fibers with different mesh sizes:(a) 80 to 120 mesh; (b) 40 to 80 mesh; (c) 20 to 40 mesh; (d) 10 to 20 mesh (33 x magnification)

The wood fibers of different sizes were placed in an electric heating constant temperature drying box (DHG-9140, Shanghai Yiheng Experimental Instrument Co., Ltd.) and dried at 105 °C for more than 8 h to ensure that the moisture content of poplar fibers was less than 3%.

High-density polyethylene (HDPE) was provided by China Petrochemical Dalian Petrochemical Company, model 5 000 s, density 0.949 to 0.953 g/L, melt index of 0.8 to 1.1 g/10 min. MAPE was provided by Tianjin Bodi Chemical Co., Ltd., and was used as coupling agent.

The raw materials, including poplar wood fibers, HDPE, and MAPE, were weighed according to the proportions provided in Table 1. In all seven WPCs groups, the composition was maintained at 60 wt% poplar wood fibers and 36 wt% HDPE. Besides, to improve the interfacial compatibility of the WPCs, MAPE was consistently added at 4 wt%.

Table 1. Mass Fraction of Fiber-reinforced HDPE Composites Made from Processing Waste from Poplar

No.	Poplar Fibers 125 to 180 μm (%)	Poplar Fibers 180 to 425 μm (%)	Poplar Fibers 425 to 850 μm (%)	Poplar Fibers 850 to 2000 μm (%)	HDPE	MAPE
WPC A	60	0	0	0	36	4
WPC B	0	60	0	0	36	4
WPC C	0	0	60	0	36	4
WPC D	0	0	0	60	36	4
WPC AD	30	0	0	30	36	4
WPC BC	0	30	30	0	36	4
WPC ABCD	15	15	15	15	36	4

Granular HDPE and MAPE were crushed into powder using an electric plant grinder. The wood fibers, HDPE powder, and MAPE powder were mixed thoroughly. The mixture was placed into a square mold measuring 160 mm × 160 mm. The mixture was laid into the mold and then put into a pressure molding machine (SL-6, Harbin Special Plastic Products Co., Ltd.). The panels were hot pressed at 180 °C for 15 min and then cold pressed for 5 min to a controlled thickness of 4 mm.

The HDPE composite reinforced with 80 to 120 mesh fibers was named WPC A, HDPE composite reinforced with 40 to 80 mesh wood fibers was named WPC B, and the composite reinforced with 20 to 40 mesh fibers and 10 to 20 mesh fibers were named C and D, respectively. From WPC A to WPC D, the mesh size of the reinforcing fibers decreased while the fiber sizes increased. The HDPE composite reinforced with a mixture of 80 to 120 mesh and 10 to 20 mesh fibers was named WPC AD, composite reinforced with a mixture of 40 to 80 mesh and 20 to 40 mesh (*i.e.*, 20 to 80 mesh) was named WPC BC, and the composite reinforced with a mixture of four mesh sizes (80 to 120 mesh, 40 to 80 mesh, 20 to 40 mesh, and 10 to 20 mesh, *i.e.*, 10 to 120 mesh) was named WPC ABCD.

Bending Mechanical Property Testing Method

The bending mechanical properties of WPCs were measured according to ASTM D 790 (2017) at room temperature of 23 ± 2 °C, with a crosshead speed of 1.9 mm/min and a span of 64 mm. The testing instrument was an electronic universal testing machine produced by Shenzhen Ruige Instrument Co., Ltd., model RGT-20A. The bending specimens were rectangular prisms with a length of 80 mm, a width of 13 mm, and a thickness of 4 mm. During the test process, the actual measured dimensions of the specimens were inputted. The results represent the average of six tests for each group.

Impact Mechanical Property Testing Method

Notched impact strength was tested using a cantilever beam pendulum impact testing machine (XJC-25, Hebei Chengde Testing Machine Co., Ltd.) according to GB/T 1043.1 (2008). The impact specimens were rectangular prisms with dimensions of 80 mm in length, 10 mm in width, and 4 mm in thickness, with no notches. During the test, the actual measured dimensions of the specimens were inputted. The testing span was 62 mm, the impact speed was 2.9 m/s, and the pendulum energy was 2 J. The results are based on eight replicates for each group.

Dynamic Thermal Mechanical Analysis Method

The dynamic thermal mechanical properties of the WPCs were determined by a dynamic mechanical analyzer produced by NETZSCH GmbH with the model DMA-242. A three-point bending mode with a frequency of 1 H was used. The temperature range was set from -80 to 120 °C, and the heating rate was 5 °C/min. Each specimen measured 40 mm in length, 10 mm in width, and 3 mm in thickness.

Creep Property Testing Method

The main instrument for creep testing was a self-made bending creep tester, as shown in Fig. 2. According to Designation D 2990 (2017), the load was applied by the three-point bending method with a span of 64 mm and a load of 5 kg of electroplated steel plate at room temperature (25±1 °C) with a relative humidity of 55% and 65%. The loading force was the weight of the steel plate (50 N) applied to the geometric center of the specimen. The bending deflection of the geometric center of the specimen in the direction of the force at different times was measured as the deformation of the material using a micrometer with a minimum scale of 0.01 mm and a range of 50 mm. The specimen dimensions were 100 mm × 40 mm × 4 mm. After 24 h loading, the load was removed and the specimen was returned freely for 24 h to observe and record the micrometer readings. Readings were taken at the following times: before loading (initial value of the micrometer), 1 s, 5 s, 10 s, 20 s, 30 s, 40 s, 50 s, 1 min, 2 min, 4 min, 6 min, 8 min, 10 min, 12 min, 30 min, 40 min, 50 min, 1 h, 2 h, 4 h, 5 h, 20 h, 24 h, and after unloading at 1 s, 5 s, 10 s, 20 s, 30 s, 40 s, 50 s, 1 min, 2 min, 4 min, 6 min, 8 min, 10 min, 12 min, 30 min, 40 min, 50 min, 1 h, 2 h, 4 h, 5 h, 20 h, and 24 h.

Fig. 2. The self-made creep test instrument

According to Designation D 2990 (2017), the conversion formula between load P and stress σ is as follows,

$$\sigma = 3PL / 2bd^2 \quad (1)$$

where σ is the stress (MPa), P is the load (N), L is the span (mm), b is the width of the specimen (mm), and d is the thickness of the specimen (mm). In the calculation, the actual measured size of the specimen was substituted.

The difference between the reading at time t and the reading of the micrometer before loading is the deformation D_t of the WPCs at time t. Similarly, according to Designation D 2990 (2017), the conversion formula between strain ε and deformation D is as follows,

$$\varepsilon = 6Dd / L^2 \quad (2)$$

where ε is the strain (mm/mm), D is the deformation (mm), L is the span (mm), and d is the thickness of the specimen (mm). In the calculation, the actual measured size of the specimen was substituted.

RESULTS AND DISCUSSION

A comprehensive analysis of the mechanical properties of WPCs reinforced with seven different specifications and combinations of wood fiber was conducted, with particular attention to their bending and impact properties (Table 2). The study examined the effects of fiber size distribution and the use of single-sized versus mixed-sized fibers on the key mechanical properties of these HDPE-based composites.

Bending Mechanical Property of WPCs

Three grades of bending properties of WPCs

According to the bending performance values, the seven kinds of WPCs were divided into three grades.

The first grade of WPCs had larger bending performance. This category of specimens included the 20 to 40 mesh fiber-reinforced HDPE composite (WPC C), the 10 to 20 mesh fiber-reinforced HDPE composite (WPC D), and the four types of uniformly mixed fiber-reinforced HDPE composite (WPC ABCD). All of these composites demonstrated bending strength exceeding 21 MPa (ranging from 21.1 to 28.1 MPa) and bending modulus greater than 2.1 GPa (ranging from 2.16 to 2.73 GPa).

The second grade of WPCs had average bending performance, including 20 to 80 mesh fiber-reinforced HDPE composite (WPC BC, with a bending strength of 15.5 MPa and a bending modulus of 2.56 GPa) and 40 to 80 mesh fiber-reinforced HDPE composite (WPC B, with a bending strength of 15.6 MPa and a bending modulus of 2.62 GPa), which had relatively similar bending properties.

The last grade of WPCs had the minimum bending performance, including 80 to 120 mesh fiber-reinforced HDPE composite (WPC A, with a bending strength of 9.41 MPa and a bending modulus of 1.58 GPa) and 80 to 120 mesh and 10 to 20 mesh mixed fiber-reinforced HDPE composite (WPC AD, with a bending strength of 11.5 MPa and a bending modulus of 1.83 GPa). There were many voids between fibers and between fibers and matrix in the two WPCs of this grade. These defects reduced the adhesion and thus affected the mechanical properties of the composites. Compared to short fibers-reinforced WPC A, the bending strength and modulus of long and short fibers-reinforced WPC AD increased 22.2% and 15.8%, respectively.

The average bending strength and modulus of the first grade WPCs were 163% and 183% higher than those of the second grade WPCs, while the average bending strength and modulus of the second grade WPCs were 48.5% and 51.9% higher than those of the third grade WPCs, respectively.

Table 2. Blending and Impact Properties of WPCs

WPCs	Size of Fibers (Mesh)	Bending Strength (MPa)	Bending Modulus (GPa)	Impact Strength (kJ/m^2)
A	80 to 120	9.41 (1.84)	1.58 (0.08)	3.07 (0.16)
B	40 to 80	15.57 (1.46)	2.62 (0.16)	6.48 (0.40)
C	20 to 40	26.71 (1.35)	2.73 (0.54)	6.88 (0.61)
D	10 to 20	21.14 (0.86)	2.31 (0.51)	6.77 (0.06)
AD	80 to 120 and 10 to 20	11.50 (0.23)	1.83 (0.18)	6.45 (0.38)
BC	20 to 80	15.49 (1.09)	2.56 (0.13)	7.75 (0.21)
ABCD	10 to 120	28.11 (1.70)	2.16 (0.09)	6.60 (0.10)

The data in brackets represent standard deviations.

Bending properties of single-species wood fibers reinforced composites

The bending strength and modulus of WPC A were the lowest. This phenomenon may be due to two aspects: first, the wood fibers of 80 to 120 mesh primarily existed in powder form, which disrupted the continuity of the fibers (see Fig. 1a), and there were numerous gaps both between the wood fibers and at the fiber-matrix interface, thereby weakening the reinforcing effect of the wood fibers on the matrix. Second, smaller fibers have a larger specific surface area (Hubbe and Grigsby 2020). While all seven WPCs groups in this study employed a fixed 4 wt% MAPE content, this constant compatibilizer dosage may have been insufficient to achieve optimal interfacial coverage for the finer fibers. Consequently, the bending strength and modulus initially increased with fiber length before showing a slight decline. This result is consistent with the findings of previous studies (Zaini *et al.* 1996; Dikobe and Luyt 2007).

When the fiber size reached 20 mesh, further increases in fiber size led to a slight decline in the bending performance of the WPC. This phenomenon mainly occurs because larger fibers tend to overlap, creating interfacial gaps between the fibers and the HDPE matrix (WPC D). These gaps weaken the bonding strength and cause stress concentration when subjected to force. WPC C (WPC with fibers of 20 to 40 mesh) achieved the optimal reinforcement effect compared to WPC D (WPC with fibers of 10 to 20 mesh), exhibiting higher bending strength and modulus values.

Bending properties of mixed-size wood fibers reinforced composites

In WPCs containing a mixture of short and long fibers, WPC AD had the lowest bending strength and modulus, positioned between WPC A and WPC D. Replacing half of the wood powder in WPC A with 10 to 20 mesh long fibers was able to increase the bending strength and modulus of WPC AD 22.2% and 15.8%, respectively. Conversely, replacing half of the long fibers in WPC D with 80 to 120 mesh wood powder resulted in a decrease in the bending strength and modulus of WPC AD of 45.6% and 20.8%, respectively. This indicates that the addition of short and long fibers had a certain effect on the bending properties of WPCs. The negative impact of adding short fibers on the bending performance of WPCs was greater than the positive effect of adding long fibers on the bending performance of WPCs.

The bending performance of WPC BC was close to that of WPC B, and in the relationship between the bending performance of WPC B, WPC C, and WPC BC, it was found that the addition of short fibers had a greater reducing effect on the bending properties of WPCs than the enhancement effect brought by the addition of long fibers.

Among the seven WPCs, WPC ABCD (reinforced with mixed fibers of four different mesh sizes) showed the highest bending strength. WPC ABCD was considered as a uniform mixture consisting of half the mass of WPC AD (mechanical properties in the third grade) and half the mass of WPC BC (mechanical properties in the second grade). Surprisingly, the mechanical properties values of WPC ABCD were classified in the first grade. Compared to WPC AD, the bending strength and modulus of WPC ABCD increased 144.4% and 18.03%, respectively. In comparison to WPC BC, the bending strength increased 81.5%, but the bending modulus decreases 15.6%. This indicates that reasonably combining fibers of different lengths and diameters can enhance the mechanical properties of HDPE composites, effectively filling the gaps between fibers and increasing the contact area with the matrix, thereby achieving better adhesion. However, the reduction of long wood fibers also adversely affected the bending modulus of the WPCs.

The Impact Mechanical Property of WPCs

The impact strengths of seven types of WPCs are listed in Table 2. Only WPC A (with 80 to 120 fiber mesh) had relatively low impact strength. The impact strength of the WPCs changed little as the mesh size of the reinforcing fibers ranging from 10 to 80. The impact strength of WPC BC with fiber mesh 20 to 80 was the highest, reaching 7.75 kJ/m^2. The other two WPCs with mixed fiber (WPC AD and WPC ABCD) had similar impact strengths. The impact strength of WPCs with mixed mesh fibers was greater than the average impact strength of WPCs with single mesh fibers of the same components. For example, the impact strength of WPC AD was greater than the average impact strength of WPC A and WPC D. This indicates that a reasonable combination of mixed mesh fiber lengths, good dispersion, mutual interweaving, and filling gaps overcomes the disadvantage of stress concentration caused by large fibers easily forming voids in the filler and matrix, while also avoiding the disadvantage of all small fibers aggregating in the matrix and failing to conduct stress.

Dynamic Thermal Mechanical Analysis of WPCs

The storage modulus curves of seven WPCs versus temperature are shown in Fig. 3. It can be seen from the figure that as the temperature increased, the storage modulus of the WPCs decreased due to the enhanced mobility of the polymer molecules at higher temperatures, leading to a reduction in the elasticity of the WPCs.

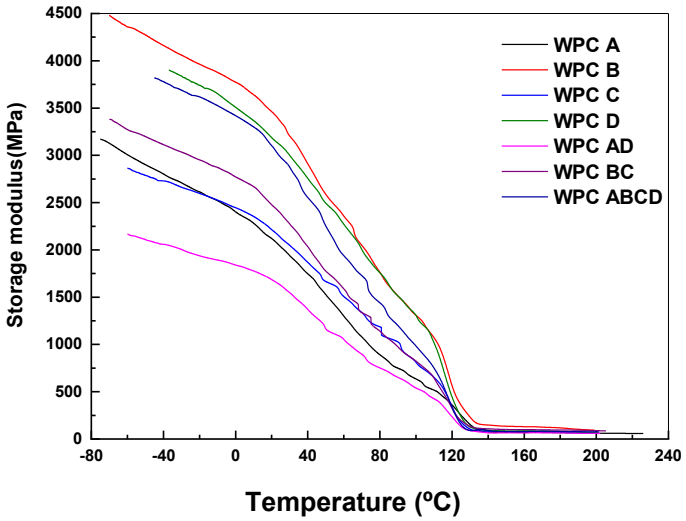

Fig. 3. Storage modulus of WPCs as a function of temperature

The storage modulus of seven types of WPCs varied the most when the temperature was -40 °C, among which, the storage modulus of WPC B (WPC with 40 to 80 mesh fibers) was the largest, differing by 2100 MPa from the storage modulus of WPC AD (WPC with mixed fibers of 80 to 120 mesh and 10 to 20 mesh), which had the lowest storage modulus. When the temperature dropped below 0 °C, the storage modulus of the WPCs decreased relatively slowly. However, when the temperature exceeded 0 °C, the storage modulus of the WPCs decreased obviously, and the differences in storage modulus among the seven WPCs diminish. When the temperature exceeded 120 °C, the difference in storage modulus among the seven WPCs became smaller, with the maximum storage modulus of WPC B differing from the minimum storage modulus of WPC AD by only 66.2 MPa, which accounts for only 3.15% of the difference at -40 °C. This indicates that fiber size has a considerable impact on the stiffness of WPCs at low temperatures, but this effect diminishes at high temperatures.

The variation of the loss modulus of seven WPCs at different temperature is shown in Fig. 4. It can be observed that as the fibers mesh size decreased, the loss modulus of the WPCs increased. When the temperature reached around 50 °C, six types of WPCs (except WPC A, which had a fiber mesh size of 80 to 120) sequentially exhibited relaxation transition peaks. At this point, the difference in loss modulus values among the WPCs reached its maximum. WPC D (with fibers mesh size of 10 to 20) exhibited the highest loss modulus, which was 247.3 MPa higher than that of WPC A, which had the lowest loss modulus. Regarding the peak temperatures, WPC B had the highest peak temperature (58.1 °C), while WPC BC had the lowest peak temperature (44.2 °C). Particularly, WPC A showed a continuous decrease in loss modulus from -80 °C to 200 °C, with only a plateau observed between -80 °C and -40 °C. This phenomenon suggests that when the wood fibers were very small or even in powder form (Fig. 1a), the energy required for the composite to melt and flow was lower compared to WPCs with larger fiber sizes.

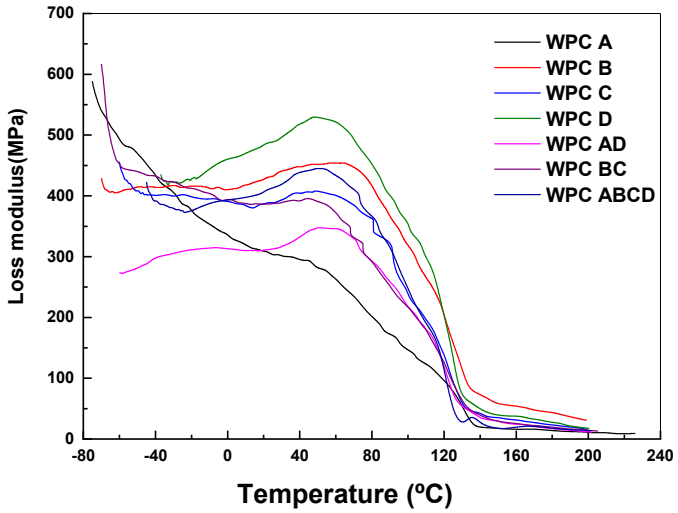

Fig. 4. Loss modulus of WPCs as a function of temperature

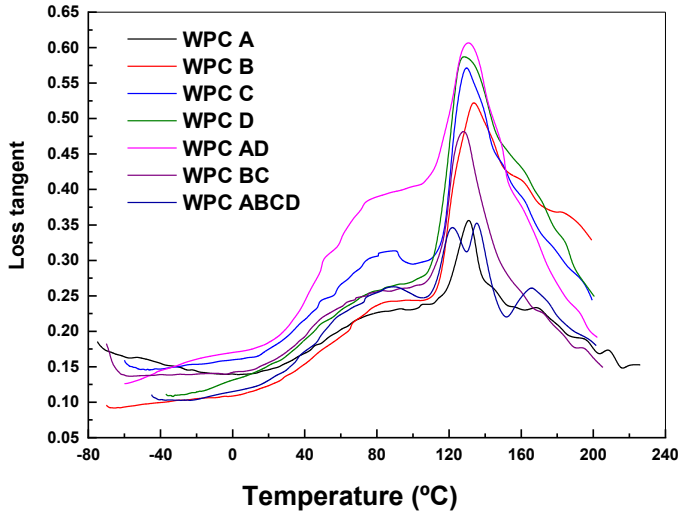

Fig. 5. Loss tangent of WPCs as a function of temperature

Table 3. Glass-Transition Temperature and the Corresponding Loss Tangent of WPCs

WPCs	Size of Fibers (Mesh)	Glass-transition Temperature (°C)	Loss Tangent
A	80 to 120	130.9	0.35633
B	40 to 80	133.8	0.52211
C	20 to 40	129.7	0.57135
D	10 to 20	128.3	0.58711
AD	80 to 120 and 10 to 20	130.8	0.60663
BC	20 to 80	128.1	0.48171
ABCD	10 to 120	135.4	0.35246

The loss tangent curves of seven WPCs *versus* temperature are shown in Fig. 5 and the glass transition temperature and the corresponding loss tangent of WPCs are shown in Table 3. Within the entire -80 to 200 ℃ range, the loss tangent value remained below 1 (within the range of [0.3 to 0.6]), with a peak appearing near 140 ℃. As the mesh size of the reinforcing fibers increased, the loss tangent values of the WPCs gradually decreased, resulting in reduced toughness and impact resistance, while the elastic characteristics became more pronounced. Previous discussion on the impact strength of WPCs also confirmed that WPC A had the poorest impact strength, while WPC C and WPC D had higher impact strength.

Creep Property of WPCs

The creep behavior of WPCs

Figure 6 shows the strain-time curves of the 24 h creep and 24 h recovery experiment conducted on seven WPCs at room temperature (25±1 °C) under conditions of 55% and 65% humidity, with a load of 50 N applied. According to the change in creep rate, the creep process can be divided into three stages, namely the initial stage, the second stage, and the final stage. The reduced creep rate in the initial stage reflected the stability of the WPCs when subjected to force, during which the WPCs experienced instantaneously recoverable elastic deformation. In the second stage, the deformation curve was linear due to an almost constant strain rate, which was considered as a transitional stage. During this time, WPCs exhibited viscoelastic and viscous deformations, with the former being time-dependent and reversible deformation, while the latter represented permanent and irreversible deformation. In the final stage, the curve should show an upward surge, as the rate of deformation tends to rise due to the material nearing failure (Xi *et al*. 2023). In this experiment, the force applied to the specimen was insufficient to cause material failure, thus the third stage did not occur.

The recovery process can be broadly divided into two distinct mechanistic stages: the initial stage and the second stage. The initial stage primarily corresponds to elastic deformation recovery, characterized by an instantaneous elastic response and a rapidly decaying recovery rate. This behavior aligns with the typical viscoelastic characteristics of polymer composites. During this stage, WPCs undergo immediate elastic recovery although the recovery rate progressively decreases over time. The second stage involves viscoelastic deformation recovery, which is not purely viscous and exhibits linear behavior with a nearly constant recovery rate. This stage partially restores the delayed elastic deformation that occurs during the secondary creep phase, while the permanent viscous flow remains irreversible (Guo and Wang 2009). The linear deformation curve in this stage reflects this fundamental recovery mechanism.

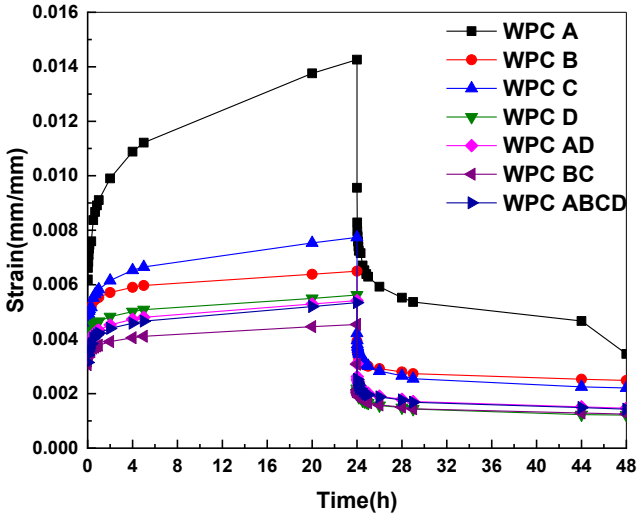

Fig. 6. 24 h creep-24 h recovery curve of WPCs at a load of 50 N

Elastic deformation of WPCs

Under a load of 50 N, the elastic deformation, 24 h deformation and 24 h recovery rates of seven WPCs are shown in Table 4.

Elastic deformation is a reversible deformation that does not change with time, also known as instantaneous deformation. In the experiment, the amount of deformation obtained by applying a load to the sample for 1 s was used for calculations (Guo and Wang 2009).

Table 4. Deformation Value of WPCs at a Load of 50 N

WPCs	Size of Fibers (Mesh)	Elastic Deformation (mm)	24 h Deformation (mm)	24 h Response Rate (%)
A	80 to 120	0.650	2.246	75.73
B	40 to 80	0.383	0.975	61.74
C	20 to 40	0.370	1.142	71.45
D	10 to 20	0.430	0.803	78.46
AD	80 to 120 and 10 to 20	0.546	0.776	72.94
BC	20 to 80	0.399	0.648	72.53
ABCD	10 to 120	0.460	0.779	73.17

For the WPCs with single mesh size fibers, as the fiber mesh size decreased, the elastic deformation of WPCs first decreased and then slightly increased. This trend was consistent with the bending mechanical test results of WPCs. Among them, the elastic deformation of WPC A (80 to 120 mesh wood fiber) was the greatest, while the elastic deformations of the other three single mesh size fibers-reinforced WPCs (WPC B, WPC C, and WPC D) were relatively similar. The elastic deformation of WPC C was less than that of the WPC D.

For the WPCs with mixed mesh size fibers, the elastic deformation of the long and short fiber mixed reinforced WPC AD was the greatest. The elastic deformation of the medium-length fibers mixed reinforced WPC BC was the smallest. The elastic

deformations of the four mixed mesh fiber-reinforced HDPE composites (WPC ABCD) are in the middle range.

24-h deformation of WPCs

For WPCs with single mesh fibers, the 24 h deformation of WPC A was markedly higher than that of the other three groups of WPCs, exhibiting the worst creep resistance, while WPC D had the smallest 24 h deformation, showing the best creep resistance. This was because the fiber size in WPC D was the largest, which can effectively maintain the continuity of the fibers (Fig. 1d) and provide good support in the matrix to achieve the best reinforcing effect. Whereas, in WPC A, the wood particles were in powder form (Fig. 1a), which disrupted the fibers' continuity, reduced the fiber strength and stiffness, and affected the reinforcement effect of the fibers, leading to a decrease in the load-bearing capacity of the composites and a reduction in creep resistance. This phenomenon is consistent with the research results of Wang *et al*. (2015), who also found that, under constant loading levels, composites containing larger diameter wood fibers exhibit better creep resistance compared to those containing smaller diameter fibers at all measured temperatures.

For WPCs with mixed mesh fibers, the creep resistance of medium and long fiber-reinforced WPC BC was superior to that of short and long fiber-reinforced WPC AD. This was attributed to the fact that the wood fibers in WPC BC were elongated (20 to 80 mesh), while WPC AD contained half of its mass as powder (80 to 120 mesh) as reinforcement material, reducing the number of rigid components provided.

Additionally, the 24 h deformation of WPCs reinforced with mixed mesh size fibers was smaller than that of those reinforced with single mesh size fibers, meaning that the 24 h creep resistance of mixed mesh size fiber reinforced composites was superior to that of single mesh size fiber-reinforced composites. The enhanced performance can be attributed to the effective combination of fiber lengths in the mixed mesh size fibers, which ensured good dispersion, mutual interweaving, and filling of gaps (WPC AD, WPC BC, and WPC ABCD). This arrangement mitigates the poor bonding effect typically observed between large fibers and the matrix, which can easily lead to voids and stress concentrations (WPC D). Furthermore, it also prevents small fibers from collecting in the matrix (WPC A), resulting in better stress transfer.

24-h response rate of WPCs

The recovery rate *R* of WPCs was equal to the ratio of the strain recovered in the creep-recovery test to the total strain of the creep.

$$R = \frac{\varepsilon_e + \varepsilon_{de}}{\varepsilon} \times 100\% = \frac{\varepsilon_e + \varepsilon_{de}}{\varepsilon_e + \varepsilon_{de} + \varepsilon_v} \times 100\% \quad (3)$$

In the Eq. 3, ε_e represents elastic strain (mm/mm), ε_{de} represents viscoelastic strain (mm/mm), ε_v represents viscous strain (mm/mm), and ε represents total strain (mm/mm).

$$\varepsilon = \varepsilon_e + \varepsilon_{de} + \varepsilon_v \quad (4)$$

Table 3 shows that the *R*-values of the three WPCs reinforced with mixed mesh size fibers were very similar after 24 h creep-24 h recovery. Among the seven WPCs, WPC D had the highest *R*, which can be verified by the results of the dynamic thermal mechanical analysis. As shown in Fig. 4, the loss tangent of WPC D was high, indicating a large viscoelastic ratio and small viscous deformation, which contributes to its elevated *R*.

Similarly, from Fig. 3, it can be concluded that the loss modulus of WPC D was the highest among the seven WPCs, further indicating that it has the lowest viscous deformation and the highest *R*. Conversely, WPC B, with a mesh size of 40 to 80, had the lowest *R*. This result can be verified by the dynamic thermal mechanical analysis results. From Fig. 2, it can be observed that the energy storage modulus of WPC D was the highest among the seven WPCs, while its *R* was relatively low.

In this experiment, the strain values of the WPCs after 24 h of unloading were minimal, ranging from 21.5% to 39.3%. This is because the load applied to the WPCs in this study were low, and therefore, elastic deformation was the predominant type of deformation during the 24 h creep period. Feng and Zhao (2022) also reported that elastic deformation was the most important deformation in the 24 h creep deformation of WPCs when the applied load was at 50% of the bending strength. Additionally, they found that the viscoelastic and viscous deformation of WPCs increased as the applied load was increased.

CONCLUSIONS

1. Both excessively large and small fiber sizes were detrimental to the improvement of the bending strength of wood-polymer composites (WPCs). The bending properties of WPC reinforced with 80 to 120 mesh fibers were the worst, while the optimal reinforcement effect was achieved with WPC reinforced with fibers ranging from 20 to 40 mesh. Increasing the fiber size beyond 20 mesh had little importance in enhancing the bending performance of the WPCs.

2. In WPCs reinforced with mixed mesh fibers, the best bending properties were found in composites containing a combination of 10 to 120 mesh fibers. This indicates that fibers with different lengths and diameters can enhance the high density polyethylene (HDPE) matrix by filling gaps between the fibers and increasing the contact area with the matrix, which helped to improve the interfacial bonding strength and mechanical properties. Adding short fibers to WPCs had a more pronounced negative impact on their bending performance compared to the addition of long fibers, which improves bending strength.

3. In terms of impact strength, WPCs with a fiber mesh size of 80 to 120 had relatively low values, as the impact strength of the WPCs did not change obviously with fiber mesh size ranging from 10 to 80. The impact strength of WPCs reinforced with a mesh size of 20 to 80 was the highest, reaching 7.75 KJ/m2. Furthermore, the impact strength of WPCs with mixed mesh fibers was greater than the average value of WPCs reinforced with single mesh fibers of the same composition.

4. As the temperature increased, the storage modulus of the WPCs decreased. As the size of wood fiber mesh increased, the loss modulus of the WPCs increased, while the loss tangent gradually decreased.

5. Under a 50N load, the 24 h creep resistance of WPCs with mixed mesh fibers was superior to that of WPCs with single mesh fibers. Among the WPCs with single mesh fibers, the best creep resistance was found in WPCs with 10 to 20 mesh fibers, while the worst performance was observed in WPCs with 80 to 120 mesh fibers. As the mesh size decreased, the 24 h recovery rate first decreased and then increased. Among WPCs with mixed mesh fibers, the best creep resistance was achieved with WPC reinforced with 20 to

80 mesh fibers, while the worst was observed in WPC with a mix of 80 to 120 mesh and 10 to 20 mesh wood fibers. The 24 h recovery rates of the three WPCs with mixed mesh fibers were similar.

ACKNOWLEDGMENTS

This research was funded by the National Natural Science Foundation of China (32160413, 32060324), 2025 Guizhou Minzu University-level Research Fund Project for Teachers(GZMUMY6), Guizhou Provincial Department of Human Resources, and Social Security high-level talent innovation and entrepreneurship project (2022-06), Department of Education of Guizhou Province (QianJiaoJi[2023]034).

REFERENCES CITED

Aref, Y., Othaman, R., Anuar, F. H., Ahmad, K. Z. K., and Baharum, A. (2018). "Superhydrophobic modification of *Sansevieria trifasciata* natural fibres: A promising reinforcement for wood plastic composites," *Polymers* 15(3), article 594. https://doi.org/10.3390/polym15030594

ASTM D790 (2017). "Standard test methods for flexural properties of unreinforced and reinforced plastics and electrical insulating materials," ASTM International, West Conshohocken, PA, USA.

ASTM D2990 (2017). "Standard test methods for tensile, compressive, and flexural creep and creep-rupture of plastics," ASTM International, West Conshohocken, PA, USA.

Ayana, K. D., Ha, C. S., and Ali, A. Y. (2024). "Comprehensive overview of wood polymer composite: Formulation and technology, properties, interphase modification, and characterization," *Sustainable Materials and Technologies* 40, article e00983. https://doi.org/10.1016/j.susmat.2024.e00983

Barbos, J. D. V., Azevedo, J. B., Cardoso, P. D. M., Garcia, F. D., and del Rio, T. G. (2020). "Development and characterization of WPCs produced with high amount of wood residue," *Journal of Materials Research and Technology* 9(5), 9684-9690. https://doi.org/10.1016/j.jmrt.2020.06.073

Bouafif, H., Koubaa, A., Perré, P., and Cloutier, A. (2009). "Effects of fiber characteristics on the physical and mechanical properties of wood plastic composites," *Composites Part A: Applied Science and Manufacturing* 40(12), 1975-1981. https://doi.org/10.1016/j.compositesa.2009.06.003

Cao, Y., Hua, X. S., Li, L. F., Wu, J., Xu, H. L. (2025). "Application of machine learning in predicting the properties of wood-plastic composites," *Journal of Guizhou University(Natural Sciences)* 42(05), 45-53. https://doi.org/10.15958/j.cnki.gdxbzrb.2025.05.05

Chaudemanche, S., Perrot, A., Pimbert, S., Lecompte, T., and Faure, F. (2018). "Properties of an industrial extruded HDPE-WPC: The effect of the size distribution of wood flour particles," *Construction and Building Materials* 162, 543-552. https://doi.org/10.1016/j.conbuildmat.2017.12.061

Dikobe, D. G., and Luyt, A. S. (2007). "Effect of filler content and size on the properties of ethylene vinyl acetate copolymer-wood fiber composites," *Journal of Applied Polymer Science* 103(6), 3645-3654. https://doi.org/10.1177/00220345850640121501

Feng, L., and Zhao, C. Y. (2022). "Analysis of creep properties and factors affecting wood plastic composites" *Polymers* 14(14), article 2814. https://doi.org/10.3390/polym14142814

GB/1043.1 (2008). "Plastics – Determination of Charpy impact properties – Part 1: Non-instrumented impact test," Standardization Administration of China, Beijing, China.

Guo, C. G., and Wang, Q. W. (2009). "Kinetics of isothermal crystallization for wood-flour polypropylene composites," *Polymer Materials Science and Engineering* 25(4), 62-65. https://doi.org/10.1145/1651587.1651601

Hassona, W., El-Kassas, A. M., and Zaafarani, N. N. (2025). "A new mixing technique in the production of wood plastic composites from recycled materials," *International Journal of Environmental Science and Technology* 22(1), 331-340. https://doi.org/10.1007/s13762-024-06137-y

Hubbe, M. A., and Grigsby, W. (2020). "From nanocellulose to wood particles: A review of particle size *vs.* the properties of plastic composites reinforced with cellulose-based entities," *BioResources* 15(1), 2030-2081. https://doi.org/10.15376/biores.15.1.2030-2081

Jeon, S., Farooq, A., Lee, I. H., Lee, D. Y., Seo, M. W., Jung, S. C., Hussain, M., Khan, M. A., Jeon, B. H., Jang, S. H., *et al.* (2024). "Green conversion of wood plastic composites: A study on gasification with an activated bio-char catalyst," *International Journal of Hydrogen Energy* 54, 96-106. https://doi.org/10.1016/j.ijhydene.2023.05.127

Khamtree, S., Srivabut, C., Khamtree, S., and Kaewmai, R. (2024). "Effects of natural fiber waste, content, and coupling agent on the physical and mechanical properties of wood species-plastic composites as green materials," *Fibers and Polymers* 25(4), 1391-1402. https://doi.org/10.1007/s12221-024-00493-9

Kim, J. W., Harper, D. P., and Taylor, A. M. (2009). "Effect of wood species on the mechanical and thermal properties of wood-plastic composites," *Journal of Applied Polymer Science* 112(3), 1378-1385. https://doi.org/10.1002/app.29522

Mital'ová, Z., Mita, D., and Berladir, K. (2024). "A concise review of the components and properties of wood–plastic composites," *Polymers* 16(11), article 1556. https://doi.org/10.3390/polym16111556

Mu, B. S., Wang, H. G., Hao, X. L., and Wang, Q. W. (2018). "Morphology, mechanical properties and dimensional stability of biomass particles/high density polyethylene composites: Effect of species and composition," *Polymers* 10(3), article 308. https://doi.org/10.3390/polym10030308

Mustafa, N., Yusuf, Y., Kudus, S. I. A., Razali, A., Sulistyarini, D. H., Halim, M. H., and Ujih, A. C. A. (2024). "The influence of MAPP and MAPE compatibilizers on physical and mechanical properties of 3D printing filament made of wood fiber/ recycled polypropylene," *Pertanika Journal of Science & Technology* 32 (S2), 77-90. https://doi.org/10.47836/pjst.32.S2.06

Na, H. N., Huang, J. C., Xu, H. G., Liu, F., Xie, L. K., Zhu, B. Q., Wang, J. C., and Zhu, J. (2023). "Structure and properties of PLA composite enhanced with biomass fillers from herbaceous plants author links open overlay panel," *Journal of Renewable Materials* 11(2), 491-503. https://doi.org/10.32604/jrm.2023.024181

Nuruzzaman, M., Shathi, A. S., Yousuf, A., Islam, M. J., Rana, M. S., Alam, M. S., Biswas, P. K., Rahman, M. A., and Mondal, M. I. H. (2025). "Composite materials from waste plastics: A sustainable approach for waste management and resource

utilization," *Polymers and Polymer Composites* 33, article 09673911251318542. https://doi.org/10.1177/09673911251318542

Qi, Z. Q., Cai, H. Z., Ren, F. Z., Liu, L., Yang, K. Y., and Han, X. S. (2024). "*In-situ* lignin regeneration strategy to improve the interfacial combination, mechanical properties and stabilities of wood-plastic composites," *Composites Science and Technology* 246, article 110366. https://doi.org/10.1016/j.compscitech.2023.110366

Rao, J. P., Zhou, Y. H., and Fan, M. Z. (2018). "Revealing the interface structure and bonding mechanism of coupling agent treated WPC," *Polymers* 10(3), article 266. https://doi.org/10.3390/polym10030266

Ratanawilai, T., and Srivabut, C. (2022). "Physico-mechanical properties and long-term creep behavior of wood-plastic composites for construction materials: Effect of water immersion times," *Case Studies in Construction Materials* 16, article e00791. https://doi.org/10.1016/j.cscm.2021.e00791

Ratanawilai, T., and Taneerat, K. (2018). "Alternative polymeric matrices for wood-plastic composites: Effects on mechanical properties and resistance to natural weathering," *Construction and Building Materials* 172, 349-357. https://doi.org/10.1016/j.conbuildmat.2018.03.266

Ribeiro, L. S., Stolz, C. M., Amario, M., da Silva, A. L. N., and Haddad, A. N. (2023). "Use of post-consumer plastics in the production of wood-plastic composites for building components: A systematic review," *Energies* 16(18), article 6549. https://doi.org/10.3390/en16186549

Wang, W. H., Huang, H. B., Du, H. H., and Wang, H. G. (2015). "Effects of fiber size on short-term creep behavior of wood fiber/HDPE composites," *Polymer Engineering & Science* 55(3), 693-700. https://doi.org/10.1002/pen.23935

Xi, F., Zhao, L. L., Wei, Y., Yi, J. Y., and Zhao, K. (2023). "Effect of temperature on the bending and creep properties of wood plastic composites," *Polymer Composites* 44(8), 4612-4622. https://doi.org/10.1002/pc.27425

Xu, J. J., Chen, C. F., Li, Y. Y., Zhou, H. Y., Hao, X. L., Ou, R. X., and Wang, Q. W. (2024). "Optimizing the rheological and mechanical properties of ultra-highly filled wood fiber/polyethylene composites through binary alloy matrix strategy," *Composites Science and Technology* 256, article 110740. https://doi.org/10.1016/j.compscitech.2024.110740

Xu, W., Corbi, O., Mapesela, S., Chen, Y., Gaff, M., and Li, H. T. (2023). "Lateral performance for wood-frame shear walls – A critical review author links open overlay panel," *Journal of Renewable Materials* 11(5), 2143-2169. https://doi.org/10.32604/jrm.2023.026773

Xue, X., Li, H. T., and Lorenzo, R. (2024). "A review of basic mechanical properties of bamboo scrimber based on small-scale specimens," *Journal of Renewable Materials* 12(4), 869-894. https://doi.org/10.32604/jrm.2024.029602

Yang, A., Liao, Z. Y., Xu, Z. S., Liu, T., Fang, Y. Q., Wang, W. H., Xu, M., Song, Y. M., Wang, Q. W., and Li, Y. (2025). "Scalable production of robust and creep resistant ultra-high filled wood-plastic composites," *Composites Part B: Engineering* 289, article 111937. https://doi.org/10.1016/j.compositesb.2024.111937

Ye, H. R., Zheng, G. Y., Zuo, S. D., Yu, Q. H., Xia, C. L., Sheng, Y. Q., Shi, Y., Wang, D. X., Li, J. Z., and Ge, S. B. (2023). "Lightweight, bacteriostatic and thermally conductive wood plastic composite prepared by chitosan modified biointerfaces," *Applied Surface Science* 615, article 156313. https://doi.org/10.1016/j.apsusc.2022.156313

Zaini, M. J., Fuad, M. Y. A., Ismail, Z., Mansor, M. S., and Mustafah, J. (1996). "The effect of filler content and size on the mechanical properties of polypropylene/oil palm wood flour composites," *Polymer International* 40(1), 51-55. https://doi.org/10.1002/(SICI)1097-0126(199605)40:1<51::AID-PI514>3.0.CO;2-I

Zhao, S. Y., Hu, F., Li, L. F., Cao, Y., Gao, H., Yang, X. H., and Xu, H. L. (2024). "Evaluation of properties of wood plastic composites made from seven types of lignocellulosic fibers," *Wood Research* 69(3), 417-431. https://doi.org/10.37763/wr.1336-4561/69.3.417431

Article submitted: May 10, 2025; Peer review completed: August 15, 2025; Revised version received: August 20, 2025; Accepted: December 18, 2025; Published: January 5, 2026.
DOI: 10.15376/biores.21.1.1564-1582